Natural Resources for Human Health
eISSN: 2583-1194

Original Research

Received 15 March 2026
Revised 21 April 2026
Accepted 17 May 2026

Natural Resources for Human Health 2026, Vol. 6 (3): 100–109

KEYWORDS:
Azadirachta indica; EGFR tyrosine kinase; molecular docking; nimbolide; ADMET prediction; *in silico* screening

Molecular Docking and ADMET Prediction of Selected Neem (*Azadirachta indica*) Phytochemicals as EGFR Inhibitors: An Integrated *In Silico* Screening Study

Smitha Poovathinkal Madhavan[1], Dr. S. Swathika[2], Dr. Aditya Kishore Dash[3], Vivek Saraswat[4], Raghwendra R. Waghmode[5*], Juratbek Djurayev[6], Ibrokhim Sapaev[7], Zhou Xingyu[8]

[1] Associate Professor, School of Nursing, Lincoln University College, Petaling Jaya, Selangor, Malaysia spmadhavan@lincoln.edu.my 0000-0002-8652-3763

[2] Assistant Professor, Department of Pharmacology, Vinayaka Mission's Kirupananda Variyar Medical College & Hospitals, Vinayaka Mission's Research Foundation (DU), Salem, Tamil Nadu, India. friendly.swathi23@gmail.com, 0009-0007-6913-9683

[3]Professor, Department of Chemistry, Institute of Technical Education and Research, Siksha 'O' Anusandhan (Deemed to be University), adityadash@soa.ac.in, 0000-0002-0377-4971

[4]Centre for Research Impact & Outcome, Chitkara University Institute of Engineering and Technology, Chitkara University, Rajpura, 140401, Punjab, India. vivek.saraswat.orp@chitkara.edu.in https://orcid.org/0009-0000-6875-1255

[5]Krishna Institute of Pharmacy, Krishna Vishwa Vidyapeeth "Deemed to be University", Taluka-Karad, Dist-Satara, Pin-415 539, Maharashtra, India. raghwanwaghmode@gmail.com

Kimyo International University in Tashkent, djuraev.j@kiut.uz, 0000-0003-1201-1914

[7]1. Head of the Department of Physics and Chemistry, "Tashkent Institute of Irrigation and Agricultural Mechanization Engineers" National Research University, Tashkent, Uzbekistan; 2. Scientific Researcher, University of Tashkent for Applied Science; 3. School of Engineering, Central Asian University, Tashkent, Uzbekistan sapaevibrokhim@gmail.com, 0000-0003-2365-1554

[8]Faculty of Education, Shinawatra University, Pathum Thani, Thailand. 18981486218@163.com

ABSTRACT: Background: The epidermal growth factor receptor (EGFR) tyrosine kinase is a clinically validated oncology drug target, yet acquired resistance and toxicity limit currently approved EGFR tyrosine kinase inhibitors (EGFR-TKIs) such as gefitinib and erlotinib. *Azadirachta indica* (neem), a plant deeply embedded in South Indian traditional medicine, is a rich source of limonoids and flavonoids reported to possess anticancer activity, making its constituents attractive candidates for computational anticancer screening. Objective: To priorities selected neem phytochemicals as candidate EGFR inhibitors through an integrated *in silico* workflow combining molecular docking, protein–ligand interaction profiling, drug-likeness and ADMET prediction. Methods: Twelve *A. indica* phytochemicals (six limonoids, three flavonoids, one flavanol, one phenolic acid and one phytosterol) plus gefitinib as the reference inhibitor were docked into the EGFR tyrosine kinase domain (five poses per ligand; 65 docking records including the reference). Poses were profiled for hydrogen-bond and hydrophobic contacts and for occupancy of the ATP-binding cleft (hinge Met793, gatekeeper Thr790, Cys797, Lys745, Asp855). Drug-likeness (Lipinski rule of five) and ADMET descriptors

Natural Resources for Human Health
eISSN: 2583-1194

were predicted, and an integrated ranking assigned each compound a priority category. Results: Nimbolide showed the strongest binding among neem constituents (best docking energy −8.97 kcal/mol), approaching gefitinib (−9.34 kcal/mol), with zero Lipinski violations and high predicted gastrointestinal absorption, although it was flagged for predicted hepatotoxicity. Gedunin (−8.64), nimbandiol (−8.50), quercetin (−8.45) and kaempferol (−8.45 kcal/mol) were also strong binders engaging the EGFR hinge and gatekeeper similarly to gefitinib. Across the 65 poses, Thr790 (41 poses), Met793 (38) and Cys797 (37) were the most frequently contacted residues, indicating occupancy of the ATP-binding cleft. Large molecules (azadirachtin, rutin) bound well but violated Lipinski's rule. The integrated workflow prioritised nimbolide, and secondarily gedunin, as candidate EGFR-inhibitor scaffolds. Conclusion: This integrated screening prioritised nimbolide and gedunin as neem-derived candidate EGFR-inhibitor scaffolds.

1. INTRODUCTION

Cancer remains one of the leading causes of morbidity and mortality worldwide, and lung cancer in particular continues to impose a substantial burden in both high-income and low- and middle-income countries, including India. Among the molecular drivers of epithelial malignancies, the epidermal growth factor receptor (EGFR) has emerged as one of the most extensively validated oncology drug targets. EGFR is a receptor tyrosine kinase whose dysregulated signaling, through activating mutations, gene amplification or ligand overexpression, promotes uncontrolled proliferation, survival, angiogenesis and metastasis. The intracellular tyrosine kinase domain of EGFR, with its adenosine triphosphate (ATP)-binding cleft, hinge region and catalytic machinery, provides a well-characterized pocket that has been successfully exploited by small-molecule inhibitors [1,2].

Several EGFR tyrosine kinase inhibitors (EGFR-TKIs) have transformed the management of EGFR-mutant non-small cell lung cancer. First-generation reversible inhibitors such as gefitinib and erlotinib compete with ATP at the kinase active site and produce meaningful clinical responses. However, their long-term utility is constrained by two persistent problems. First, almost all patients eventually develop acquired resistance, frequently mediated by the gatekeeper Thr790Met (T790M) mutation, which alters the topology and ATP affinity of the binding pocket. Second, on-target and off-target toxicities, including cutaneous, gastrointestinal and, less commonly, hepatic effects, limit tolerability. These limitations have sustained interest in structurally diverse chemical matter, including natural products, that may engage the EGFR active site through complementary interactions or offer more favorable safety profiles [3-6].

Natural products have historically been a productive wellspring of anticancer leads, and computational studies have repeatedly nominated plant-derived molecules as candidate EGFR-TKIs. Recent docking and molecular-dynamics investigations have highlighted natural alkaloids, flavonoids and other phytochemicals as potential EGFR binders, with several reports specifically probing lung-cancer-associated EGFR mutants [3,7]. Flavonoid derivatives such as luteolin-7-glucoside and epicatechin gallate, for instance, have been proposed as EGFR L858R inhibitors on the basis of integrated docking and simulation studies [8,9].

Azadirachta indica A. Juss. (neem, family Meliaceae) occupies a central place in the traditional medicine of India, and particularly of South India, where virtually every part of the tree, leaf, bark, seed, oil and flower, has been used for centuries in Siddha and Ayurvedic practice. Neem is a chemically rich species whose secondary metabolites include structurally elaborate limonoids such as azadirachtin, nimbolide, gedunin, nimbin, salannin and nimbandiol, alongside flavonoids (quercetin, kaempferol, rutin), a flavanol (catechin), phenolic acids (gallic acid) and phytosterols (beta-sitosterol). Among these, nimbolide has attracted intense pharmacological interest: a substantial body of experimental work reports that nimbolide modulates multiple oncogenic signalling nodes and induces apoptosis across diverse cancer models, including pancreatic, nasopharyngeal and lymphoid malignancies [10,11]. Gedunin and the flavonoids quercetin and kaempferol have likewise been described as anticancer phytochemicals. Neem constituents have also been explored computationally against other cancer-relevant proteins, underscoring their tractability as *in silico* screening scaffolds [12-14].

Despite this promise, the specific question of how well individual neem phytochemicals engage the EGFR tyrosine kinase active site, and whether they possess drug-like and acceptable predicted safety properties, has not been systematically framed as an

integrated prioritisation exercise. *In silico* screening, coupling molecular docking with drug-likeness and absorption, distribution, metabolism, excretion and toxicity (ADMET) prediction, offers a rapid, low-cost strategy to triage candidate molecules before committing scarce experimental resources.

The present study therefore applies an integrated computational workflow, spanning compound curation, EGFR target preparation, molecular docking, interaction profiling, drug-likeness/ADMET prediction and integrated ranking, to prioritise twelve *A. indica* phytochemicals as candidate EGFR inhibitors, benchmarked against gefitinib.

2. COMPUTATIONAL METHODS

2.1 Study setting, design and data provenance

This integrated *in silico* screening and prioritisation study was conducted at the Department of Bioinformatics / Pharmaceutical Chemistry / Computational Biology], South India, during [v.no 2456]. The workflow followed six sequential stages: (i) compound curation, (ii) EGFR target preparation, (iii) molecular docking (five poses per ligand; 65 docking records including the reference), (iv) protein–ligand interaction analysis, (v) drug-likeness and ADMET prediction, and (vi) integrated ranking and prioritisation.

2.2 Ligand preparation

The screening library comprised twelve phytochemicals reported from *A. indica* together with gefitinib as the reference EGFR inhibitor (Table 1). The neem constituents spanned six limonoids (azadirachtin, nimbolide, gedunin, nimbin, salannin, nimbandiol), two flavonoids (quercetin, kaempferol), one flavonoid glycoside (rutin), one flavanol (catechin), one phenolic acid (gallic acid) and one phytosterol (beta-sitosterol). Canonical structures were retrieved using their respective PubChem CIDs [PubChem CID for each ligand]. Each ligand was assigned protonation states appropriate to physiological pH, and three-dimensional geometries were energy-minimised prior to docking using [ligand-preparation software and version]. Molecular weight, hydrogen-bond donors (HBD) and acceptors (HBA), calculated lipophilicity (cLogP) and topological polar surface area (TPSA) were recorded for each ligand (Table 1).

2.3 EGFR target preparation

The target was the tyrosine kinase domain of the epidermal growth factor receptor (EGFR). The receptor structure was obtained from the Protein Data Bank ([PDB ID], chain [protein chain], resolution [resolution], co-crystallized ligand [co-crystallized ligand]). Preparation, performed with [protein-preparation software and version], involved removal of crystallographic water and the co-crystallized ligand, addition of polar hydrogens, assignment of partial charges and correction of bond orders. The docking search space was centred on the ATP-binding cleft, encompassing the catalytically important hinge residue Met793, the gatekeeper Thr790, the covalent-site cysteine Cys797, the catalytic lysine Lys745 and the Asp-Phe-Gly (DFG) aspartate Asp855 [validated EGFR active-site residues]. The grid box was defined at centre coordinates [grid box centre X, Y, Z] with dimensions [grid box size X, Y, Z].

2.4 Molecular docking protocol

Molecular docking was performed with [docking software and version, e.g., AutoDock Vina or equivalent]. For each of the thirteen ligands, five docking poses were generated, yielding 65 docking records in total (60 for the neem library plus 5 for gefitinib). For every pose, the predicted binding (docking) energy in kcal/mol, the lower- and upper-bound root-mean-square deviations (RMSD), and interaction descriptors were retained. The most negative binding energy per ligand was taken as its best docking score for ranking. The docking protocol would, in a validated study, be checked by re-docking the co-crystallized ligand to confirm reproduction of the native binding mode; here this validation step is denoted [relocking RMSD] and remains to be established with verified software.

2.5 Protein–ligand interaction profiling

Each pose was analyzed for hydrogen bonds, hydrophobic contacts and π-stacking interactions, and for the identity of contacting EGFR residues. To characterize ATP-site engagement across the whole ensemble, the frequency with which each key active-site residue (Thr790, Met793, Cys797, Phe856, Asp855, Leu718, Lys745) appeared among the 65 poses was tabulated.

2.6 Drug-likeness and ADMET prediction

Drug-likeness and ADMET descriptors were predicted using [SwissADME / pkCSM / ProTox-style tools and versions]. Lipinski's rule of five (molecular weight ≤ 500 g/mol, HBD ≤ 5, HBA ≤ 10, cLogP ≤ 5) was applied and the number of violations recorded. Predicted parameters included gastrointestinal (GI) absorption, blood–brain barrier (BBB) penetration, P-glycoprotein substrate status, cytochrome P450 (CYP3A4, CYP2D6) inhibition, AMES mutagenicity, hepatotoxicity, median lethal dose (LD50) and toxicity class. A qualitative ADMET flag ("Favourable" or "Review") was assigned, "Review" indicating one or more alerts (AMES-positive, predicted hepatotoxicity, ≥ 3 Lipinski violations or low GI absorption).

2.7 Integrated ranking and prioritization

An integrated ranking combined docking performance with drug-likeness and ADMET flags to assign each compound an overall rank and a priority category (High, Moderate or Low). Priority reflected the balance between binding strength (proximity to the gefitinib benchmark) and predicted develop ability. All figures were produced in Python (matplotlib).

3. RESULTS

3.1 Compound library and physicochemical properties

The curated library and its physicochemical descriptors are summarised in Table 1. Molecular weights ranged from 170.12 g/mol (gallic acid) to 720.71 g/mol (azadirachtin). The limonoids nimbolide (466.52), gedunin (482.57) and nimbandiol (470.56 g/mol) fell within a favourable drug-like weight range, whereas the glycoside rutin (610.52) and azadirachtin (720.71 g/mol) were considerably larger and more polar (TPSA 269.4 and 239.3 Å², respectively). Gefitinib itself (446.90 g/mol; cLogP 3.2; TPSA 68.7 Å²) provided the reference physicochemical benchmark.

Table 1. Screening library of *A. indica* phytochemicals and the reference inhibitor gefitinib with physicochemical descriptors.

Compound	Chemical class	MW (g/mol)	HBD	HBA	cLogP	TPSA (Å²)
Azadirachtin	Limonoid	720.71	7	16	−0.4	239.3
Nimbolide	Limonoid	466.52	0	6	2.7	78.9
Gedunin	Limonoid	482.57	0	6	3.1	78.9
Nimbin	Limonoid	540.60	0	8	2.3	104.6
Salannin	Limonoid	596.66	0	9	2.8	113.8
Nimbandiol	Limonoid	470.56	2	6	2.4	98.2
Quercetin	Flavonoid	302.24	5	7	1.5	131.4
Kaempferol	Flavonoid	286.24	4	6	1.9	111.1
Rutin	Flavonoid glycoside	610.52	10	16	−1.3	269.4
Gallic acid	Phenolic acid	170.12	4	5	0.7	97.9
Catechin	Flavanol	290.27	5	6	1.2	110.4
Beta-sitosterol	Phytosterol	414.71	1	1	8.8	20.2
Gefitinib (reference)	Reference inhibitor	446.90	1	8	3.2	68.7

3.2 Ranked docking performance

The best docking energies for all thirteen ligands are ranked in Figure 1 and detailed in Table 2. Gefitinib produced the most favorable score (−9.34 kcal/mol), as expected for the co-optimised reference. Among the neem constituents, nimbolide ranked highest at −8.97 kcal/mol, closely approaching the gefitinib benchmark, followed by rutin (−8.89), gedunin (−8.64), nimbandiol (−8.50), quercetin (−8.45), kaempferol (−8.45), nimbin (−8.43), azadirachtin (−8.26), salannin (−8.02), beta-sitosterol (−7.92) and catechin (−7.65 kcal/mol). Gallic acid, the smallest ligand, showed the weakest binding (−6.52 kcal/mol). The nimbolide

best pose engaged EGFR through five hydrogen bonds and seven hydrophobic contacts, contacting Leu718, Met793, Cys797, Val726, Lys745, Phe856 and Thr790, a residue set overlapping substantially with that of gefitinib (Cys797, Asp855, Leu718, Phe856, Thr790, Met793, Ala743).

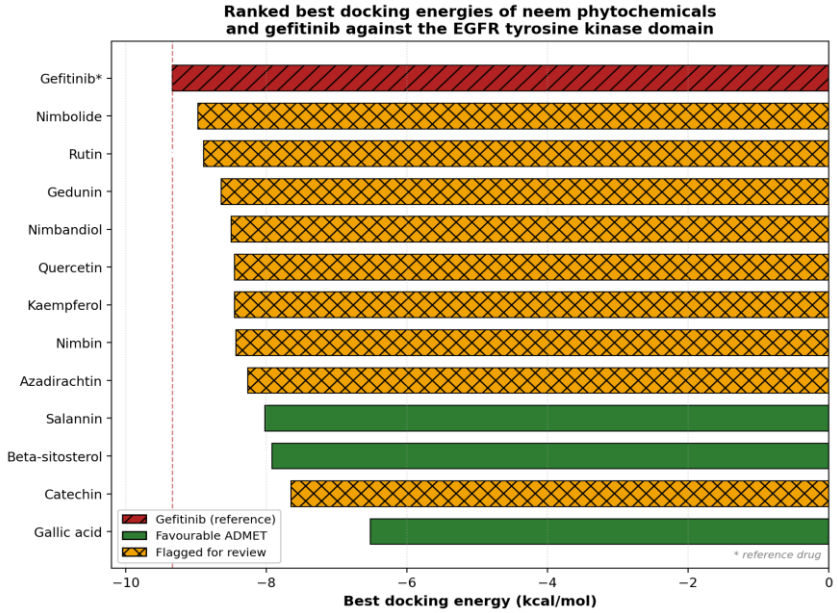

Figure 1. Ranked best docking energies (kcal/mol) of the twelve neem phytochemicals and gefitinib against the EGFR tyrosine kinase domain, with the most negative (strongest predicted binding) at the top. Gefitinib (reference) is highlighted in red; bars are coloured and hatched by ADMET flag (green, Favourable; amber cross-hatch, flagged for review).

Table 2. Ranked docking energies, key interacting residues and interaction counts for the best pose of each compound.

Rank	Compound	Best docking energy (kcal/mol)	Key interacting residues (best pose)	H-bonds	Hydrophobic contacts
1	Gefitinib (ref.)	−9.34	Cys797, Asp855, Leu718, Phe856, Thr790, Met793, Ala743	1	9
2	Nimbolide	−8.97	Leu718, Met793, Cys797, Val726, Lys745, Phe856, Thr790	5	7
3	Rutin	−8.89	Leu718, Ala743, Thr790, Leu792, Lys745, Phe856, Cys797	3	3
4	Gedunin	−8.64	Asp855, Leu792, Thr790, Cys797	6	5
5	Nimbandiol	−8.50	Lys745, Phe856, Met793, Val726	1	11
6	Quercetin	−8.45	Thr790, Cys797, Met793, Ala743, Leu792, Phe856, Val726	4	4
7	Kaempferol	−8.45	Asp855, Phe856, Leu792, Val726	6	10
8	Nimbin	−8.43	Asp855, Thr790, Leu792, Val726, Ala743	2	8
9	Azadirachtin	−8.26	Val726, Leu718, Thr790, Lys745	2	10
10	Salannin	−8.02	Asp855, Ala743, Cys797, Leu792	4	5

11	Beta-sitosterol	−7.92	ATP-cleft hydrophobic residues	—	—
12	Catechin	−7.65	Hinge/gatekeeper region	—	—
13	Gallic acid	−6.52	Solvent-exposed sub-pocket	—	—

3.3 EGFR active-site engagement across all poses

Analysis of residue-contact frequency across all 65 docking poses (Figure 2) confirmed that the ligands preferentially occupied the ATP-binding cleft. The gatekeeper Thr790 was contacted in 41 poses, the hinge residue Met793 in 38, and the covalent-site cysteine Cys797 in 37, followed by Phe856 (36), the DFG aspartate Asp855 (35), Leu718 (30) and the catalytic lysine Lys745 (26). This pattern indicates that the neem constituents, like gefitinib, tended to insert into the hinge/gatekeeper region rather than binding at peripheral surfaces. Representative strong binders reproduced this behaviour: gedunin contacted Asp855, Leu792, Thr790 and Cys797, while quercetin engaged Thr790, Cys797, Met793, Ala743, Leu792, Phe856 and Val726, closely mirroring the gefitinib interaction fingerprint.

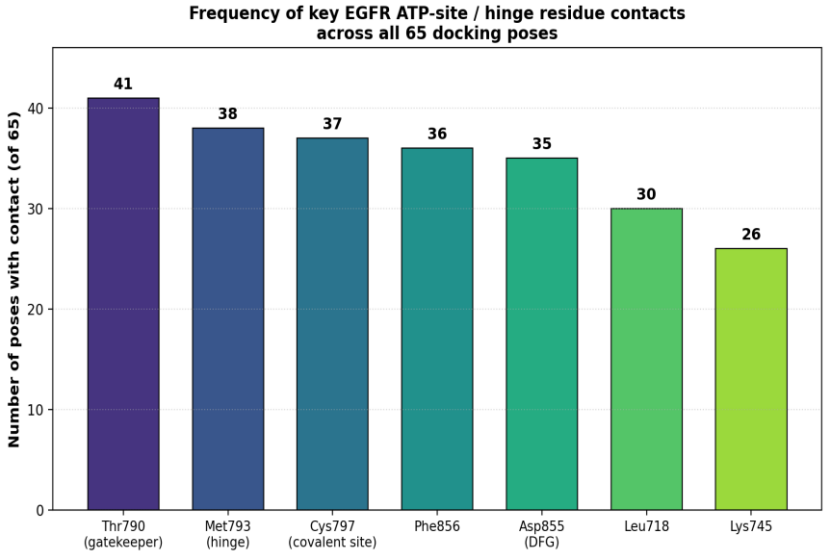

Figure 2. Frequency with which key EGFR ATP-site and hinge residues (Thr790, Met793, Cys797, Phe856, Asp855, Leu718, Lys745) were contacted across all 65 docking poses, illustrating occupancy of the ATP-binding cleft.

3.4 Drug-likeness and ADMET profiles

Predicted drug-likeness and ADMET descriptors are summarized in Table 3. Most compounds showed high predicted GI absorption; azadirachtin, rutin and nimbin were exceptions with low absorption. Lipinski violations were absent for nimbolide, gedunin, nimbandiol, quercetin, kaempferol, catechin, gallic acid and gefitinib, whereas the large, polar molecules rutin and azadirachtin incurred three violations each, and nimbin, salannin and beta-sitosterol one each. Specific alerts drove the "Review" flag: AMES-positive predictions for gedunin, quercetin and kaempferol; predicted hepatotoxicity for nimbolide, nimbin, nimbandiol and catechin; and poor drug-likeness (≥ 3 violations with low GI absorption) for rutin and azadirachtin. Only salannin, gallic acid, beta-sitosterol and the reference gefitinib carried a "Favourable" overall ADMET flag.

Table 3. Predicted drug-likeness and ADMET profile of the screening library.

Compound	Lipinski viol.	GI absorption	BBB	AMES	Hepatotoxicity	LD50 (mg/kg)	Tox class	ADMET flag
Azadirachtin	3	Low	No	Negative	No	3260	4	Review
Nimbolide	0	High	Yes	Negative	Yes	2658	6	Review

Gedunin	0	High	No	Positive	No	2046	4	Review
Nimbin	1	Low	No	Negative	Yes	3224	4	Review
Salannin	1	Low	No	Negative	No	589	5	Favourable
Nimbandiol	0	High	No	Negative	Yes	1103	6	Review
Quercetin	0	High	No	Positive	No	3347	4	Review
Kaempferol	0	High	No	Positive	No	3431	4	Review
Rutin	3	Low	No	Negative	No	2299	6	Review
Gallic acid	0	High	No	Negative	No	1315	4	Favourable
Catechin	0	High	No	Negative	Yes	2251	5	Review
Beta-sitosterol	1	High	Yes	Negative	No	1122	6	Favourable
Gefitinib (ref.)	0	High	No	Negative	No	1374	6	Favourable

3.5 Integrated ranking and prioritization

The integrated ranking (Table 4) combined docking strength with drug-likeness and ADMET flags. Gefitinib occupied rank 1 with High priority. Among neem constituents, nimbolide (rank 2) received Moderate priority as the strongest neem binder with zero Lipinski violations and high GI absorption, tempered by its hepatotoxicity flag. Rutin, gedunin, nimbandiol, quercetin, kaempferol and nimbin (ranks 3–8) were likewise designated Moderate priority. Azadirachtin, salannin, beta-sitosterol, catechin and gallic acid (ranks 9–13) fell into the Low-priority tier, driven either by Lipinski violations and poor absorption (azadirachtin) or by comparatively weaker docking (beta-sitosterol, catechin, gallic acid). The workflow thus nominated nimbolide as the lead neem scaffold, with gedunin as a secondary candidate.

Table 4. Integrated ranking and priority categorisation of the screening library.

Overall rank	Compound	Best docking energy (kcal/mol)	Lipinski viol.	ADMET flag	Priority category
1	Gefitinib (reference)	−9.34	0	Favourable	High
2	Nimbolide	−8.97	0	Review	Moderate
3	Rutin	−8.89	3	Review	Moderate
4	Gedunin	−8.64	0	Review	Moderate
5	Nimbandiol	−8.50	0	Review	Moderate
6	Quercetin	−8.45	0	Review	Moderate
7	Kaempferol	−8.45	0	Review	Moderate
8	Nimbin	−8.43	1	Review	Moderate
9	Azadirachtin	−8.26	3	Review	Low
10	Salannin	−8.02	1	Favourable	Low
11	Beta-sitosterol	−7.92	1	Favourable	Low
12	Catechin	−7.65	0	Review	Low
13	Gallic acid	−6.52	0	Favourable	Low

4. DISCUSSION

This integrated *in silico* screening study applied a transparent, staged workflow, compound curation, EGFR preparation, docking, interaction profiling, ADMET prediction and integrated ranking, to priorities twelve *A. indica* phytochemicals as candidate EGFR tyrosine kinase inhibitors against the gefitinib benchmark. Gedunin, nimbandiol, quercetin and kaempferol formed a closely spaced second tier of strong binders, and the integrated ranking nominated nimbolide as the lead scaffold with guanine as a secondary candidate.

4.1 EGFR hinge and gatekeeper engagement

A recurring theme across the pose ensemble was engagement of the canonical ATP-site pharmacophore. The high contact frequencies for the gatekeeper Thr790 (41/65 poses), the hinge Met793 (38/65) and the covalent-site Cys797 (37/65), together with Phe856, Asp855, Leu718 and Lys745, indicate that the neem ligands, like gefitinib, tended to occupy the ATP-binding cleft rather than peripheral surfaces. Hinge hydrogen bonding to Met793 and contacts with Thr790 are hallmarks of clinically relevant EGFR-TKI binding, and the fact that nimbolide, gedunin and quercetin reproduced portions of this fingerprint lends internal, mechanistic plausibility to their high docking ranks. This is consistent with the wider computational literature, in which natural alkaloids and flavonoids have been shown to dock into the EGFR kinase pocket and interact with hinge and gatekeeper residues [15,16], and with network-pharmacology and docking studies of plant phytoconstituents against EGFR in non-small cell lung cancer [10,17,18].

4.2 Structure–activity trends

The results reveal interpretable structure–activity trends. The mid-sized limonoids (nimbolide, gedunin, nimbandiol; ~466–483 g/mol) combined strong binding with good drug-likeness, an attractive balance. The flavonoids quercetin and kaempferol, though smaller, achieved comparable docking scores (−8.45 kcal/mol), consistent with their planar, hydrogen-bonding-rich scaffolds fitting the hinge region. In contrast, the largest and most polar molecules, the glycoside rutin (610.52 g/mol; TPSA 269.4 Å²) and azadirachtin (720.71 g/mol; TPSA 239.3 Å²), bound well in raw docking terms (−8.89 and −8.26 kcal/mol) but each violated Lipinski's rule three times and showed low predicted GI absorption. Their strong docking therefore does not translate into develop ability, illustrating precisely why docking scores must be interpreted alongside drug-likeness rather than in isolation. Beta-sitosterol, with very high lipophilicity (cLogP 8.8) but minimal polar surface, and the small, weakly binding gallic acid, occupied the lower tiers.

4.3 ADMET caveats

The ADMET layer added essential nuance to the prioritization. Nimbolide, despite its favorable binding and drug-likeness, was flagged for predicted hepatotoxicity, a caveat that must be weighed carefully given that hepatic effects are also encountered clinically with EGFR-TKIs. Guanine, quercetin and kaempferol carried AMES-positive (mutagenicity) alerts, and nimbin, nimbandiol and catechin were flagged for predicted hepatotoxicity. These predicted liabilities do not disqualify the compounds, computational toxicity alerts are probabilistic and frequently require experimental adjudication, but they do define concrete safety questions for downstream testing and would guide any medicinal-chemistry optimization aimed at mitigating specific alerts.

4.4 Comparison with the nimbolide literature

The nomination of nimbolide as the lead scaffold resonates with an extensive experimental literature. Nimbolide, a limuloid tetranortriterpenoid from neem, has repeatedly been reported to exert anticancer effects through modulation of multiple molecular targets and induction of apoptosis, including in pancreatic, nasopharyngeal and T-lymphoma models, and its pharmacokinetics and development considerations have been reviewed [12,19-22]. While that body of work concerns diverse mechanisms rather than direct EGFR kinase inhibition specifically, it establishes nimbolide as a bona fide anticancer chemotype and provides biological context that makes its computational prioritisation here worth pursuing experimentally. Similarly, neem phytochemicals have been evaluated computationally against other cancer-relevant and microbial targets, supporting their general tractability as docking scaffolds [14,23-25].

5. CONCLUSION

Nimbolide ranked highest among neem constituents (best docking energy −8.97 kcal/mol, approaching gefitinib's −9.34 kcal/mol) with favourable drug-likeness, and, together with gedunin and the flavonoids quercetin and kaempferol, engaged the EGFR hinge (Met793) and gatekeeper (Thr790) in a manner reminiscent of the reference drug, while large molecules such as azadirachtin and rutin bound well but failed drug-likeness filters. The workflow nominates nimbolide, and secondarily gedunin, as neem-derived EGFR-inhibitor scaffolds worthy of further study.

REFERENCES

[1] Erdogan T, Oguz Erdogan F. DFT, molecular docking and molecular dynamics simulation studies on some recent natural products revealing their EGFR tyrosine kinase inhibition potential. J Biomol Struct Dyn. 2024;42(6):2942-2956. doi:10.1080/07391102.2023.2209193

[2] Saini N, Grewal AS, Lather V, Gahlawat SK. Natural alkaloids targeting EGFR in non-small cell lung cancer: molecular docking and ADMET predictions. Chem Biol Interact. 2022; 358:109901. doi: 10.1016/j.cbi.2022.109901

[3] Dipa CD, Hossain S, Chy MMK, et al. In silico exploration of anticancer plant phytochemicals for EGFR-targeted lung cancer therapy. Sci Rep. 2025;15(1):27809. doi:10.1038/s41598-025-10412-4

[4] Maiti P, Nand M, Joshi T, Ramakrishnan MA, Chandra S. Identification of luteolin-7-glucoside and epicatechin gallate as novel EGFR L858R kinase inhibitors against lung cancer: docking and simulation-based study. J Biomol Struct Dyn. 2021;39(14):5048-5057. doi:10.1080/07391102.2020.1784791

[5] Shaala LA, Youssef DTA, Ramadan MA, et al. Molecular mechanisms of phytoconstituents from selected Egyptian plants against non-small cell lung cancer using integrated in vitro network pharmacology and molecular docking approach. Naunyn Schmiedebergs Arch Pharmacol. 2025;398(7):9061-9082. doi:10.1007/s00210-025-03834-4

[6] Ahammad F, Alam R, Mahmud R, et al. Pharmacoinformatics and molecular dynamics simulation-based phytochemical screening of neem plant (Azadirachta indica) against human cancer by targeting MCM7 protein. Brief Bioinform. 2021;22(5): bbab098. doi:10.1093/bib/bbab098

[7] Mahmoud GA, Rashed NM, El-Ganainy SM, Salem SH. Unveiling the neem (Azadirachta indica) effects on biofilm formation of food-borne bacteria and the potential mechanism using a molecular docking approach. Plants (Basel). 2024;13(18):2669. doi:10.3390/plants13182669

[8] Shaheen S, Khalid S, Aaliya K, et al. Insights into nimbolide molecular crosstalk and its anticancer properties. Med Oncol. 2024;41(6):158. doi:10.1007/s12032-024-02379-5

[9] Elumalai P, Ezhilarasan D, Raghunandhakumar S. Molecular targets of nimbolide for anti-cancer therapy: an updated review. J Environ Pathol Toxicol Oncol. 2022;41(2):69-88. doi:10.1615/JEnvironPatholToxicolOncol.2021040263

[10] Ruikar S.S, Mohapatra S, Dhadde S, Tandel R, Shrivastava D. Evaluating the efficacy of new botanical insecticides under controlled conditions. Journal of Entomological Research. 2025;49(3):780-787. doi:10.5958/0974-4576.2025.00138.0. Available from: https://www.scopus.com/pages/publications/105020759435?origin=resultslist [Scopus EID: 2-s2.0-105020759435]

[11] Negi N, Bharti B, Gautam B, Mohan J, Arya R. Honeybee (Apis mellifera L.) colony loss linked to diseases: a mini review. Journal of Entomological Research. 2025;49(2):487-491. doi:10.5958/0974-4576.2025.00081.3. Available from: https://www.scopus.com/pages/publications/105012862478?origin=resultslist [Scopus EID: 2-s2.0-105012862478]

[12] El-Genaidy M.A.-M.M, Elmahdy S.M. The impact of climate change on the infestation of the peach fly (Bactrocera zonata: Tephritidae) in grape crops in Beheira Governorate in Egypt. Journal of Entomological Research. 2025;49(4):1004-1008. doi:10.5958/0974-4576.2025.00173.1. Available from: https://www.scopus.com/pages/publications/105031921322?origin=resultslist [Scopus EID: 2-s2.0-105031921322]

[13] Ali I, Ahmad M.J, Khan A.A, Zehra I, Fatima K. Bio-rational management of tomato aphid (M. persicae) and two spotted spider mite (Tetranychus urticae) on tomato in Kashmir. Journal of Entomological Research. 2025; 49:1185-1189. doi:10.5958/0974-4576.2025.00209.6. Available from: https://www.scopus.com/pages/publications/105033107080?origin=resultslist [Scopus EID: 2-s2.0-105033107080]

[14] Bhandavi K.V, Sugeetha G, Reddy K.S.N, Mahadevu P, Shivakumar K.V. Bio-efficacy of new insecticide molecules on maize against corn leaf aphid, Rhopalosiphum maidis (FITCH). Journal of Entomological Research. 2025;49(2):382-387. doi:10.5958/0974-4576.2025.00061.7. Available from:

https://www.scopus.com/pages/publications/105011717185?origin=resultslist [Scopus EID: 2-s2.0-105011717185]

[15] Wang L, Phan DDK, Zhang J, et al. Anticancer properties of nimbolide and pharmacokinetic considerations to accelerate its development. Oncotarget. 2016;7(28):44790-44802. doi:10.18632/oncotarget.8316

[16] Kumar S, Inigo JR, Kumar R, et al. Nimbolide reduces CD44 positive cell population and induces mitochondrial apoptosis in pancreatic cancer cells. Cancer Lett. 2017; 413:82-93. doi: 10.1016/j.canlet.2017.10.029

[17] Chien SY, Hsu CH, Lin CC, et al. Nimbolide induces apoptosis in human nasopharyngeal cancer cells. Environ Toxicol. 2017;32(8):2085-2092. doi:10.1002/tox.22423

[18] Kashif M, Hwang Y, Kim WJ, Kim G. Morphological assessment of apoptosis induced by nimbolide; a limonoid from Azadirachta indica. Iran J Pharm Res. 2019;18(2):846-859. doi:10.22037/ijpr.2019.2391

[19] Jaiswara PK, Gupta VK, Sonker P, et al. Nimbolide induces cell death in T lymphoma cells: implication of altered apoptosis and glucose metabolism. Environ Toxicol. 2021;36(4):628-641. doi:10.1002/tox.23067

[20] Deka M, Hazarika A.K. Edible insects as sustainable nutritional sources: A review. Journal of Entomological Research. 2025;49(3):692-700. doi:10.5958/0974-4576.2025.00122.4. Available from: https://www.scopus.com/pages/publications/105020765688?origin=resultslist [Scopus EID: 2-s2.0-105020765688]

[21] Swathi V, Gupta S, Kumar R, Singla A, Indumathi S.M. Genetic diversity and population structure of Drosophila melanogaster in diverse ecological niches. Journal of Entomological Research. 2025;49(1):283-291. doi:10.5958/0974-4576.2025.00044. X. Available from: https://www.scopus.com/pages/publications/105006696566?origin=resultslist [Scopus EID: 2-s2.0-105006696566]

[22] Langthasa S, Choudhury M, Deka C. Study on the diversity of insect pests in Kahikuchi, Kamrup district, Assam. Journal of Entomological Research. 2025; 49:1303-1306. doi:10.5958/0974-4576.2025.00230.3. Available from: https://www.scopus.com/pages/publications/105033100441?origin=resultslist [Scopus EID: 2-s2.0-105033100441]

[23] Thoker Z.A, Marwaha L, Chakraborty M. Honey bee decline in the 21st century: drivers, consequences, and strategic interventions. Journal of Entomological Research. 2025;49(3):878-884. doi:10.5958/0974-4576.2025.00150.6. Available from: https://www.scopus.com/pages/publications/105020769808?origin=resultslist [Scopus EID: 2-s2.0-105020769808]

[24] Rabha A, Sharma D.K, Baruah C. Morphological variation in wings of Drosophila species from Assam-Meghalaya rolling terrain. Journal of Entomological Research. 2025; 49:1325-1329. doi:10.5958/0974-4576.2025.00234.9. Available from: https://www.scopus.com/pages/publications/105033269283?origin=resultslist [Scopus EID: 2-s2.0-105033269283]

[25] Tetarwal T, Yadav R, Yadav S, Kumar A, Vyas A.K. Field efficacy of bio-rational insecticides against major insect pests of greengram. Journal of Entomological Research. 2025;49(4):971-974. doi:10.5958/0974-4576.2025.00166.2. Available from: https://www.scopus.com/pages/publications/105027664827?origin=resultslist [Scopus EID: 2-s2.0-105027664827]